

## ROLE OF CD133 MOLECULE IN WNT RESPONSE AND RENAL REPAIR

Alessia Brossa<sup>1\*</sup>, Elli Papadimitriou<sup>1\*</sup>, Federica Collino, Danny Incarnato<sup>3,4</sup>, Salvatore Oliviero<sup>3,4</sup>, Giovanni Camussi<sup>2</sup> and Benedetta Bussolati<sup>1</sup>

<sup>1</sup>Department of Biotechnology and Health Sciences, Molecular Biotechnology Center, University of Turin, Via Nizza 52, 10126 Torino Italy

<sup>2</sup>Department of Medical Sciences; University of Turin, Cso Dogliotti 14, 10126 Torino Italy.

<sup>3</sup> Italian Institute for Genomic Medicine (IIGM), Via Nizza 52, 10126 Torino, Italy.

<sup>4</sup> Dipartimento di Scienze della Vita e Biologia dei Sistemi, University of Turin, Via Accademia Albertina, 13, Torino, Italy.

**Running title:** Role of CD133 in renal tubular cells.

**Correspondence:** Benedetta Bussolati, Molecular Biotechnology Centre, University of Torino, via Nizza 52, 10126 Torino, Italy. Tel. 011-6706453, Fax. 011-6631184, e-mail: [benedetta.bussolati@unito.it](mailto:benedetta.bussolati@unito.it).

## **Supplementary Materials and Methods.**

### **Sorting and labeling of CD133<sup>+</sup> and CD133<sup>-</sup> RPCs.**

To recover CD133<sup>+</sup> and CD133<sup>-</sup> cells, the single cell suspension of RPCs (passage #4) underwent magnetic separation for CD133 (Mylteni, CD133 Cell Isolation Kit, containing the anti-CD133/1 mAb, clone AC133). CD133<sup>+</sup> and CD133<sup>-</sup> cells were re-suspended in DMEM (LONZA) without serum at a concentration of 10<sup>6</sup> viable cells/ml, and stained with DIO- or DIL-Vybrant cell-labeling solutions (Molecular Probes) respectively, according to manufacturer's instructions. DIO- and DIL- labeled RPCs were then mixed in the proportion of 88% DIO-CD133<sup>+</sup> and 12% DIL-CD133<sup>-</sup> RPCs (corresponding to the proportion observed in the unfractionated RPCs population). Cells were then plated in expansion medium (Endothelial Basal Medium (EBM) plus supplement kit; CambrexBioScience) at density 1\*10<sup>4</sup> and subjected to cisplatin damage. The percentage of DIO-CD133<sup>+</sup> and DIL-CD133<sup>-</sup> RPCs was evaluated by cytofluorimetric analysis both in basal conditions and 48h and one week after cisplatin-treatment. Labeled cells were also maintained in single culture and CD133 expression was analyzed at the indicated time points.

**Supplementary Table I.** Primers used in the study.

<b>Gene ID</b>	<b>Forward primer</b>	<b>Reverse primer</b>
<b>GAPDH</b>	5'-TGG AAG GAC TCA TGA CCA CAG T-3'	5'-CAT CAC GCC ACA GTT TCC C-3'
<b>CD133</b>	5'-CCA TGG CAA CAG CGA TCA -3'	5'-GGC TAG TTT TCA CGC TGG TCA -3'
<b>PAX2</b>	5'-ATG GAT ATG CAC TGC AAA GCA GA-3'	5'-CTA GTG GCG GTC ATA GGC AG-3'
<b>VCAM1</b>	5'-GGC AGA GTA CGC AAA CAC TTT ATG-3'	5'-AAA GCC CTG GCT CAA GCA T-3'
<b>FOXD1</b>	5'-ACC CTC AGC ACT GAG ATG TC-3'	5'-CCA CGT CGA TGT CTG TTT CC-3'
<b>SOX9</b>	5'-CAA GCT CTG GAG ACT TCT GAA CG-3'	5'-AGA TGT GCG TCT GCT CCG T-3'
<b>Wnt4</b>	5'- CTC ATG AAC CTC CAC AAC AAT GAG-3'	5'-CTC GCC AGC ACG TCT TTA CC- 3'
<b>36B4</b>	5'-CAG CAA GTG GGA AGG TGT AAT CC- 3'	5'-CCC ATT CTA TCA TCA ACG GGT ACA A - 3'
	<b>Tel1</b>	<b>Tel2</b>
<b>Telomerase</b>	5'-CGG TTT GTT TGG GTT TGG GTT TGG GTT TGG GTT TGG GTT- 3'	5'-GGC TTG CCT TAC CCT TAC CCT TAC CCT TAC CCT TAC CCT- 3'

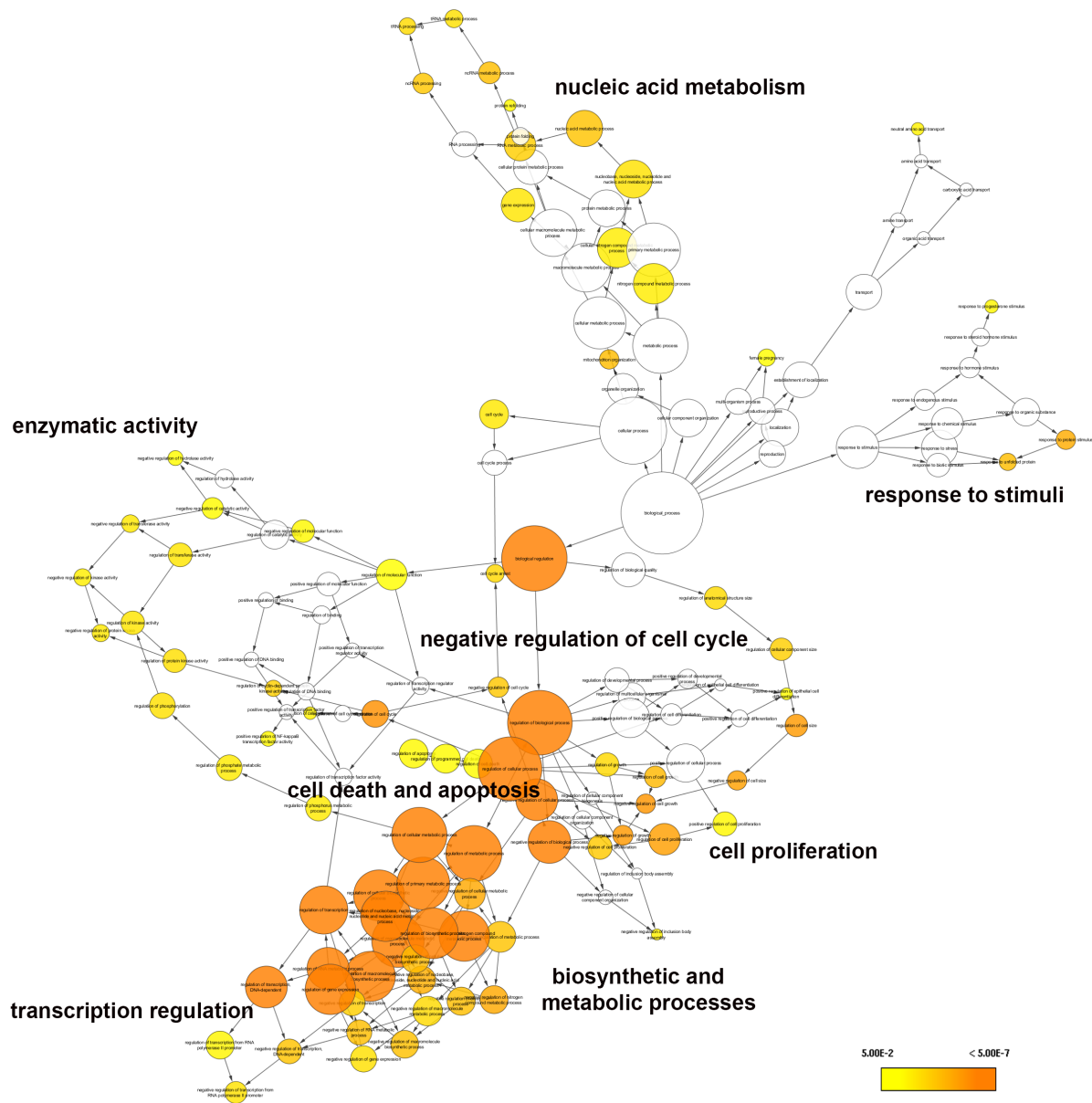
**Supplementary Table II. Differential gene modulation in CD133-Kd cells.** List of the genes differentially modulated by cisplatin treatment in shPROM1/2 cells vs GFP cells (Fold change:  $\log_2(\text{CIS shPROM1/2} / \text{CIS GFP}) \leq -1$  or  $\geq 1$ ) ordered as ascending values. Fold change between control cisplatin treated and untreated cells (CIS GFP vs GFP) and CD133-Kd treated and untreated cells (shPROM1/2 CIS vs shPROM1/2) are also reported in the first columns.

Symbol	Gene name	CIS vs CTR Fold change		Difference in shPROM vs GFP
		GFP	shPROM	
SGK3	serum/glucocorticoid regulated kinase family member 3	-1.75	-13.31	-11.59
PROM1	Prominin 1	-1.01	-1.54	-1.91
WNT7A	Wnt family member 7A	-1.42	-2.06	-1.89
RAD51B	RAD51 paralog B	-1.43	-2.80	-1.66
C3orf67	chromosome 3 open reading frame 67	-1.59	-3.15	-1.26
COL6A3	collagen type VI alpha 3 chain	-1.77	-1.11	-1.13
ZNF438	Zinc finger protein 438	-2.03	-2.92	-1.10
GLI3	GLI family zinc finger 3	-3.76	-4.16	-1.07
MIPOL1	mirror-image polydactyly 1	-1.96	-3.53	-1.05
RPL36A-HNRNPH2	RPL36A-HNRNPH2 readthrough	1.03	-0.25	-1.04
PRKAR2B	protein kinase cAMP-dependent type II regulatory subunit beta	-1.19	-1.29	-1.01
CCDC8	coiled-coil domain containing 8	-1.12	-0.70	1.02
NCRNA00185	TTY14 testis-specific transcript, Y-linked 14	-1.35	-0.75	1.04
AHRR	aryl-hydrocarbon receptor repressor	-1.94	-0.27	1.06
HECW1	HECT, C2 and WW domain containing E3 ubiquitin protein ligase 1	-3.33	-2.55	1.07
ANKMY1	ankyrin repeat and MYND domain containing 1	-1.71	-0.23	1.08
PELI2	pellino E3 ubiquitin protein ligase family member 2	-2.99	-1.69	1.08
MGC23284	SNAI3-AS1 SNAI3 antisense RNA 1	-1.38	0.19	1.09
MILR1	Mast cell immunoglobulin like receptor 1	-1.29	0.48	1.12
POLE2	DNA polymerase epsilon 2, accessory subunit	-2.41	-0.52	1.18
RUSC1-AS1	RUSC1 antisense RNA 1 [Homo sapiens]	-3.41	-0.55	1.18
LOC100129917	Uncharacterized LOC100129917	-1.35	0.07	1.19

TTY14	Testis-specific transcript, Y-linked 14	-1.97	0.01	1.23
PCDHGB4	Protocadherin gamma subfamily B, 4	-1.08	-0.32	1.29
PCDHGB1	protocadherin gamma subfamily B, 1	-1.80	-0.78	1.32
THSD7A	thrombospondin type 1 domain containing 7A	-5.96	-3.80	1.36
SETBP1	SET binding protein 1	-4.43	-2.91	1.37
PRH1-PRR4	PRH1-PRR4 readthrough	-1.99	-0.19	1.39
FSBP	fibrinogen silencer binding protein	-2.55	-0.29	1.40
LOC100507218	RNF157 antisense RNA 1	-1.93	-0.14	1.41
SRGAP2P2	SLIT-ROBO Rho GTPase activating protein 2B	-3.52	-1.77	1.42
PCDHGB3	protocadherin gamma subfamily B, 3	-1.87	-0.27	1.43
HNF4A	Hepatocyte nuclear factor 4 alpha	-4.57	-2.77	1.44
TRPV4	transient receptor potential cation channel subfamily V member 4	-2.69	-0.92	1.45
SRGN	serglycin	-1.08	0.35	1.46
NUDT4P1	Nudix hydrolase 4 pseudogene 1	-1.77	1.01	1.54
AJAP1	Adherens junctions associated protein 1	-3.44	-2.10	1.54
PPM1H	protein phosphatase, Mg <sup>2+</sup> /Mn <sup>2+</sup> dependent 1H	-5.38	-3.28	1.56
NPFF	neuropeptide FF-amide peptide precursor	-1.97	0.35	1.58
AP4S1	Adaptor related protein complex 4 sigma 1 subunit	-2.98	-0.87	1.66
TNFSF18	TNF superfamily member 18	-3.29	-0.36	1.68
CTSL3	ccathepsin L family member 3, pseudogene	-1.29	2.18	1.68
CADPS2	calcium dependent secretion activator 2	-4.68	-2.61	1.78
LOC100505549	uncharacterized LOC100505549	-2.83	-0.99	1.80
PDE4D	phosphodiesterase 4D	-6.19	-4.02	1.93
LTB	Lymphotoxin Beta	-2.52	0.11	1.96
RBMS3	RNA binding motif single stranded interacting protein 3	-5.61	-3.22	2.09
PRDM5	PR/SET domain 5	-3.55	-1.29	2.10
SAA2-SAA4	SAA2-SAA4 readthrough	-1.52	1.03	2.12
C2orf82	Chromosome 2 open reading frame 82	-2.55	1.35	2.24
RAB19	RAB19, member RAS oncogene family	-3.14	1.03	2.50
LOC400927	cTPTE and PTEN homologous inositol lipid phosphatase pseudogene	-1.97	1.57	2.79
IDH1-AS1	IDH1 antisense RNA 1	-1.97	1.02	2.94
SNURF	SNRPN upstream reading frame	-3.21	0.33	2.96
SLC10A7	solute carrier family 10 member 7	-5.61	-2.62	3.11
KRTAP5-2	keratin associated protein 5-2	-4.21	0.72	3.98
H3F3A	H3 histone family member 3A	-11.02	-0.03	11.07
CORO7-PAM16	CORO7-PAM16 readthrough	-14.60	-3.11	11.70

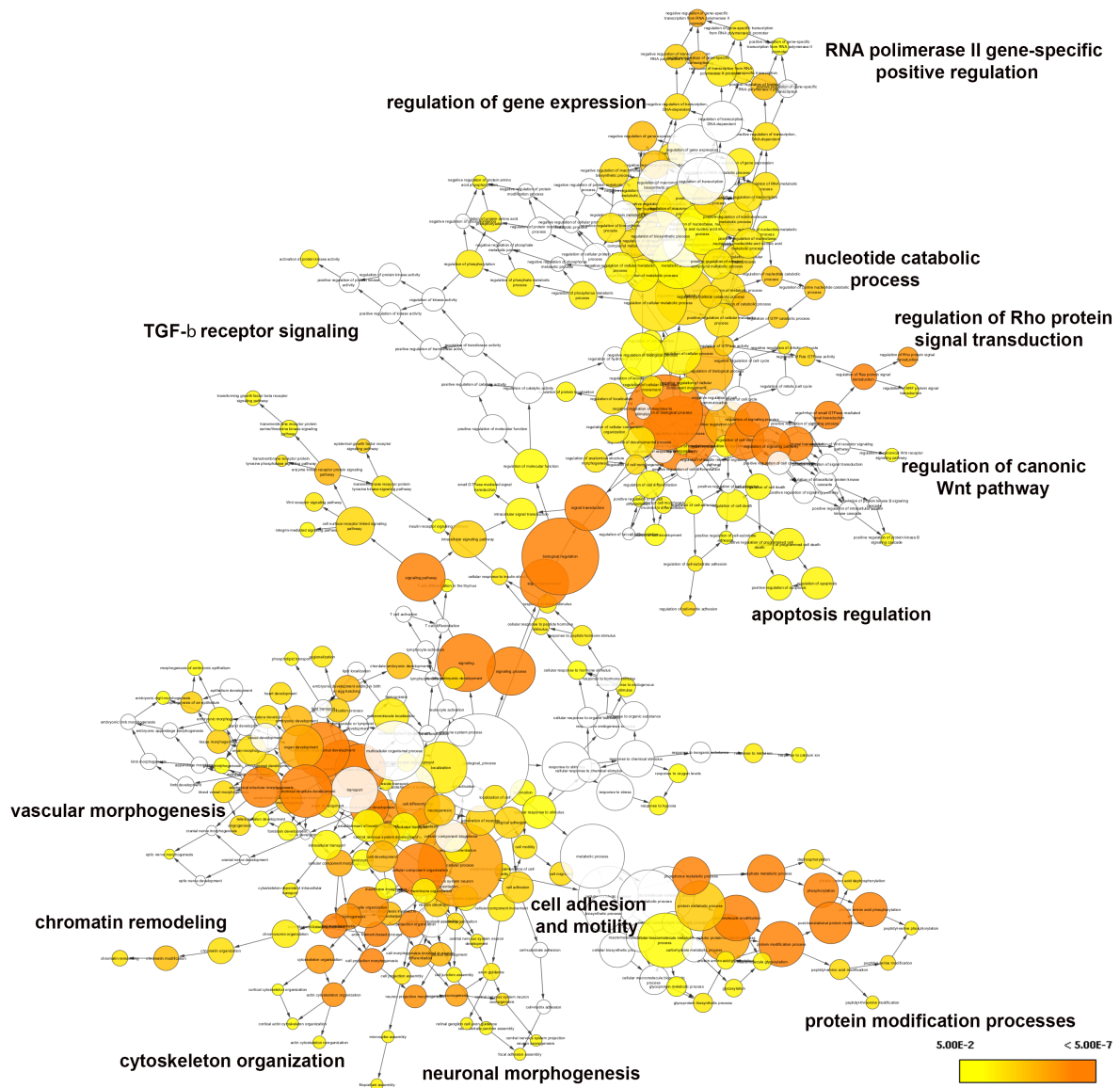
NPPA-AS1	NPPA antisense RNA 1	-14.59	-2.21	12.06
LOC100240734	uncharacterized LOC100240734	-14.50	0.74	12.63
MYLK-AS1	MYLK antisense RNA 1	-15.03	-0.51	13.41
C20orf196	chromosome 20 open reading frame 196	-14.87	-0.60	13.97
ZFP91-CNTF	ZFP91-CNTF readthrough (NMD candidate)	-14.43	0.83	14.94
RNF5	ring finger protein 5	-14.91	-0.21	15.29
CECR5-AS1	HDHD5 antisense RNA 1	-14.94	15.38	15.38
LOC728066	family with sequence similarity 133 member D, pseudogene	-14.46	1.48	15.70
RMRP	RNA component of mitochondrial RNA processing endoribonuclease	-15.94	0.56	17.22
RNU6ATAC	RNA, U6atac small nuclear (U12-dependent splicing)	-19.35	-1.01	18.28

## Supplementary Figures



**Supplementary Figure 1.**

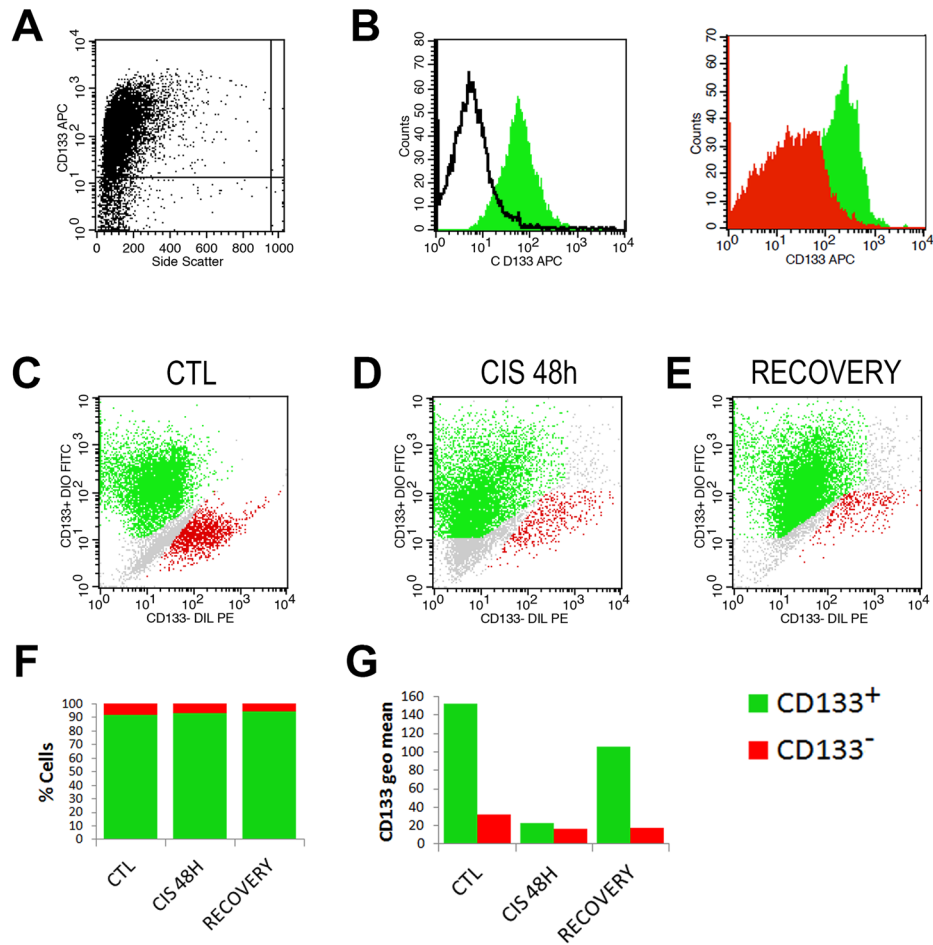
**BiNGO gene ontology analysis of the biological processes over-represented by the genes upregulated in cisplatin treated CD133<sup>+</sup> cells (n=964 genes) ( $p \leq 0.05$ , see the color bar). Node colors represent the statistical significance. The following biological processes were defined: nucleic acid metabolism, transcription regulation, response to stimuli, cell cycle and proliferation, regulation of enzymatic activities and cell death processes.**



**Supplementary Figure 2.**

**BiNGO gene ontology analysis of the biological processes over-represented by the genes downregulated in cisplatin treated CD133<sup>+</sup> cells (n=1521 genes) ( $p \leq 0.05$ , see the color bar). Node colors represent the statistical significance. The following biological processes were overrepresented: gene expression, chromatin remodeling, nucleotide catabolic process, cytoskeleton organization, vascular and neuronal morphogenesis, cell motility and Rho signal transduction, canonic Wnt signaling and TGF-beta receptor signaling.**





### Supplementary Figure 3.

Cytofluorimetric analysis of RPCs showing the percentage of cells expressing CD133 in basal conditions (A), and after immunomagnetical sorting (B). Green and red filled area shows CD133 expression in CD133<sup>+</sup> and CD133<sup>-</sup> cell fraction respectively. Black line shows isotype binding. C-E: Cytofluorimetric analysis showing CD133<sup>+</sup> (green) and CD133<sup>-</sup> (red) RPCs in basal conditions (CTL) (C), 48 hours (CIS 48H) (D) and seven days (RECOVERY) after cisplatin treatment (E). F: Ratio of the percentage of CD133<sup>+</sup> (green) and CD133<sup>-</sup> (red) RPCs in CTL), 48 hours (CIS 48H) and seven days (RECOVERY) after cisplatin treatment. G: Geometric mean of CD133-APC fluorescence intensity was measured in CD133<sup>+</sup> (green) and CD133<sup>-</sup> (red) RPCs (in single cultures) in basal conditions (CTL), 48 hours (CIS 48H) and seven days (RECOVERY) after cisplatin treatment.